Organic Electronics 13 (2012) 925–931

Contents lists available at SciVerse ScienceDirect

Organic Electronics

journal homepage: www.elsevier.com/locate/orgel

Letter

Enhancing the efficiency of simplified red phosphorescent organic light emitting diodes by exciton harvesting

Y.-L. Chang, Z.B. Wang *, M.G. Helander, J. Qiu, D.P. Puzzo, Z.H. Lu

Department of Materials Science and Engineering, University of Toronto, 184 College St., Toronto, Ontario, Canada M5S 3E4

ARTICLE INFO

Article history:
Received 14 September 2011
Received in revised form 15 December 2011
Accepted 29 January 2012
Available online 22 February 2012

Keywords:
Phosphorescent organic light emitting diodes
Energy transfer
Exciton harvesting
Carrier trapping
Co-doping

ABSTRACT

High efficiency red phosphorescent organic light emitting diode (PHOLED) employing co-doped green emitting molecule bis(2-phenylpyridine)(acetylacetonate)iridium(III) [Ir(p-py)$_2$(acac)] and red emitting molecule bis(2-methyldibenzo[f,h]quinoxaline)(acetylacetonate)iridium(III) [Ir(MDQ)$_2$(acac)] into 4,4′-bis(carbazol-9-yl)biphenyl (CBP) host in a simplified wide-bandgap platform is demonstrated. The green molecule is shown to function as an exciton harvester that traps carriers to form excitons that are then efficiently transferred to the Ir(MDQ)$_2$(acac) by triplet-to-triplet Dexter energy transfer, thereby significantly enhancing red emission. In particular, a maximum current efficiency of 37.0 cd/A and external quantum efficiency (EQE) of 24.8% have been achieved without additional out-coupling enhancements. Moreover, a low efficiency roll-off with the EQE remaining as high as 20.8% at a high luminance of 5000 cd/m^2 is observed.

1. Introduction

Significant progress on the development of phosphorescent organic light emitting diodes (PHOLEDs) has been made over the past decade [1–5], which eventually led to the recent commercialization of active-matrix organic light-emitting diode (AMOLED) displays. Nevertheless, devices with much higher efficiencies over a wide luminance range (10–5000 cd/m^2) are still in demand for cost-competitive general lighting and low power consumption LED backlight applications. In particular, among the three primary colors, red PHOLEDs are currently lagging behind green and blue PHOLEDs [1,3,5–8] in terms of device performance presumably due to the energy gap law, which states that non-radiative rate constant increases with the reduction of the energy gap, leading to a lower emission quantum yield [2]. There are thus very few reports of red PHOLEDs exhibiting high external quantum efficiency (EQE) of >20% [2,9].

In order to reduce the driving voltage and enhance the emission efficiency of red PHOLEDs, several research groups have taken the approach of developing new bipolar host materials and dopant systems with improved carrier mobility and charge balance in the emissive layer (EML) [10–12]. Su et al. recently developed a series of bipolar host materials with heterocyclic cores to reach an EQE of 17.6% at a luminance of 100 cd/m^2 [8]. Chien et al. reported the use of a fluorene-based bipolar host material to obtain an EQE of 18.6% at 1000 cd/m^2 [11]. More recently, Fan et al. have developed a tetraphenylsilane-based bipolar host material together with a narrow linewidth deep red dopant to yield a very high EQE of 24.0% at 1000 cd/m^2 [9].

Alternatively, high efficiency red PHOLEDs can be realized using standard materials by a careful design of the device architecture to balance charge carriers, confine excitons in the EML [3,13–15] and minimize various quenching processes such as triplet–triplet annihilation [16,17] and triplet–polaron quenching [18]. Jou et al. inserted a thin (10 nm) di-[4-(*N*,*N*-ditolyl-amino)-phenyl] cyclohexane (TAPC) layer next to the EML to modulate excessive hole-injection and confine the electrons within the EML, thereby balancing the injection of both carriers

* Corresponding author.
E-mail addresses: zhibin.wang@utoronto.ca (Z.B. Wang), zhenghong.lu@utoronto.ca (Z.H. Lu).

1566-1199/$ - see front matter © 2012 Elsevier B.V. All rights reserved.
doi:10.1016/j.orgel.2012.01.026

and obtaining a high EQE of 19.8% at 1000 cd/m^2 [13]. Meerheim et al. demonstrated *p-i-n* red PHOLED by doping the electron and hole transporting layers and incorporating electron/hole blocking layers to achieve an EQE of 20% at 100 cd/m^2 [14]. More recently, Jou et al. employed double EMLs sandwiched by electron/hole injection and transport layers to obtain a high EQE of 20.3% at 100 cd/m^2 [15]. Despite improved performances, these approaches naturally increase device complexity and cost considerably, rendering them less attractive for commercial applications.

In this article, we demonstrated a simplified red PHOLED with high EQE of >20% over a broad luminance range (10–5000 cd/m^2) by using the standard red emitter bis(2-methyldibenzo[f,h]quinoxaline)(acetylacetonate)iridium(III) [Ir(MDQ)$_2$(acac)]. The green emitter bis(2-phenylpyridine)(acetylacetonate)iridium(III) [Ir(ppy)$_2$(acac)] was co-doped along with the red emitter to significantly boost device performance. In particular, we have achieved a maximum EQE of 24.8%, which remained as high as 20.8% at a high luminance of 5000 cd/m^2, which represents the highest device performance using standard and readily available red phosphors. We also systematically studied the exciton harvesting and found that carrier trapping and direct exciton formation on the green emitter followed by efficient triplet-to-triplet Dexter energy transfer to the red emitter are the keys to the high efficiency of our devices.

2. Results and discussion

2.1. Device performance and optimization

A schematic diagram of our simplified device structure and the corresponding energy-level diagram are depicted in Fig. 1, where TPBi [2,2′,2″-(1,3,5-benzinetriyl)-tris(1-phenyl-1-*H*-benzimidazole)] serves as the electron transport layer (ETL) and CBP [4,4′-bis(carbazol-9-yl)biphenyl] functions as both the hole transport layer (HTL) and the host. The EML consists of co-evaporated green emitter (G) Ir(ppy)$_2$(acac) and red emitter (R) Ir(MDQ)$_2$(acac) [19] with various doping concentrations into the CBP host. All doping concentrations reported in this work are by weight percentage. One of the key features of our design is the use of wide-bandgap and high triplet energy ETL, HTL and host materials that can effectively confine generated excitons in the EML [4]. There are also noticeably very small energy barriers between the ETL and HTL, i.e., there is only ~0.1 eV difference in the highest occupied molecular orbital (HOMO) level and lowest unoccupied molecular orbital (LUMO) level between the two materials, which effectively prevents significant charge accumulation at the ETL/HTL interface that could induce various quenching processes [20].

Fig. 2a shows the current efficiency versus luminance (CE–L) plot of the PHOLED devices at a fixed red doping concentration (2%) and varied green doping concentrations (from 0% to 12%). It is clear that the co-doped devices show progressively better performance with reduced efficiency roll-off at lower green doping concentrations as a result of minimized self-quenching [21]. For the optimized device with 2% doping each, we achieve a high current efficiency (power efficiency) of 37.0 cd/A (30.2 lm/W), 35.3 cd/A (21.7 lm/W), and 31.0 cd/A (15.7 lm/W) at 100 cd/m^2, 1000 cd/m^2, and 5000 cd/m^2, respectively. These correspond to an impressive EQE of 24.8%, 23.7%, and 20.8% at 100 cd/m^2, 1000 cd/m^2, and 5000 cd/m^2, respectively.

Since the improved efficiency is achieved in a co-doped system, efficiency may potentially be contributed in part by the green emission. Therefore, in order to illustrate that the high performance is primarily due to the dramatic enhancement of the red emission and not the green, the absolute irradiance of the corresponding devices at a current density of 10 mA/cm^2 was measured as shown in Fig. 2b. The spectra are characterized by a dominant emission peak at 606 nm from the red emitter (over 20 times stronger than the green emission peak at 515 nm), i.e., the emission is mainly contributed by one emitter (red) rather than both [22]. Moreover, we observe distinct red emission enhancement at all green doping levels with a maximum improvement of ~1.75 times at 2% green doping over the solely red doped device. It is worth noting that there is a slight red shift of the spectrum with the incorporation of high green doping concentration, i.e., the red peak shifts from 606 nm at 2% to 609 nm at 12% green doping concentration, possibly due to aggregation of the emitter [23].

The results shown in Fig. 2 clearly demonstrate that the co-doped green phosphor can significantly enhance red emission. However, it may be arguable that the solely red doped device has not yet been optimized, i.e., a different doping concentration may also enhance the red emission efficiency. Therefore, we conducted a comprehensive study on the performance of the devices under a wide range of red and green doping concentrations. The EQEs of which at a luminance of 1000 cd/m^2 are summarized in Fig. 3a. Without any green doping, the red doped device exhibits the highest EQE of only 17.3% at 4% doping concentration. The highest EQE device was realized at 2% red and 2% green doping, which is equivalent to ~1.35 times that of the optimized solely red doped device (see Fig. 3b). The inset of Fig. 3b shows the electroluminescence (EL) spectra of the optimized co-doped device, which remain stable under a wide range of current densities with constant Commission Internationale de l'Eclairage (CIE) coordinates of (0.61, 0.39).

2.2. Device working mechanism: exciton harvesting and energy transfer

To acquire an in-depth understanding of the operating principle governing these devices, we first examined the dominant energy transfer processes taking place in the EML (schematically drawn in the inset of Fig. 4) by comparing the room temperature absorption spectra of Ir(ppy)$_2$(acac) and Ir(MDQ)$_2$(acac), as well as the photoluminescence (PL) spectra of CBP and Ir(ppy)$_2$(acac) as shown in Fig. 4. The considerable overlap of the CBP emission spectrum with the absorption spectra of both Ir(ppy)$_2$(acac) and Ir(MDQ)$_2$(acac) suggests effective Förster and/or Dexter energy transfer from the host to both guest molecules. Due to the presence of the heavy metal Ir atom in the emitters, intersystem crossing (ISC) from the singlet charge transfer state to the triplet metal ligand charge transfer state (^{3}MLCT) occurs

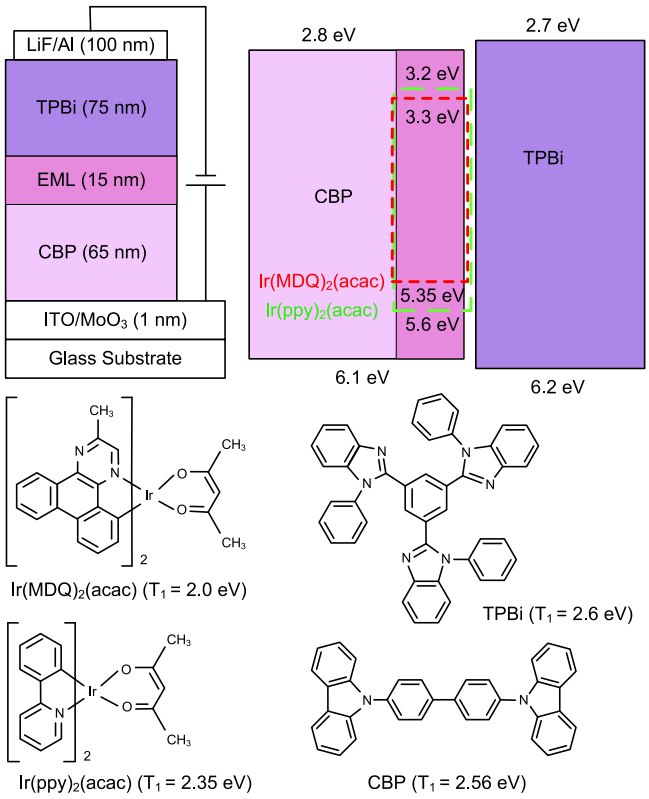

Fig. 1. Schematic device structure and corresponding energy-level diagram of the devices considered in this work as well as the molecular structure and triplet energies (T_1) of the materials used. The EML consists of co-evaporated Ir(ppy)$_2$(acac) and Ir(MDQ)$_2$(acac) with various doping concentrations by weight% into CBP.

rapidly for both emitters [24,25]. More importantly, the substantial phosphorescent emission spectrum overlap of Ir(ppy)$_2$(acac) with the ^{3}MLCT absorption of Ir(MDQ)$_2$(acac) (at ~525 nm) implies that efficient Dexter energy transfer from the triplet state of the green emitter to the triplet state of the red emitter is highly favorable. We note that energy transfer from the singlet states of Ir(ppy)$_2$(acac) to the singlet states of Ir(MDQ)$_2$(acac) is also possible, however, cannot be dominant due to the efficient ISC process of each emitter.

To shed more light on the energy transfer process, we examined the normalized EL spectra at a fixed green doping level of 2% under a range of red doping levels as shown in Fig. 5. We observe an increase in green emission intensity with the reduction of red doping (inset), which can be attributed to the saturation of the red triplet emission sites by the excitons from the green emitter [26]. This is expected since the Dexter energy transfer occurs on a much faster time scale than the excited state lifetime of the phosphors [27,28]. It is worth noting that the observed blue shift arises from red doping concentration reduction, resulting in a reduced aggregation [19], similar to the trend observed for our devices without any green doping.

As shown above, there is efficient energy transfer from the green to the red phosphor. We might therefore conclude that the incorporation of green dopants can enhance the red emission by exciting an increased number of red triplet emissive sites. However, if this is the case then why cannot a similarly high efficiency be achieved by simply increasing the doping concentration of the solely red doped device?

To address this question, we first eliminated the electrical effects, such as carrier trapping by the green phosphors, by comparing the absolute PL quantum efficiency (η_{PL}) of an isolated CBP thin film (100 nm in thickness) doped with various Ir(ppy)$_2$(acac) and Ir(MDQ)$_2$(acac) concentrations. The quantum efficiencies were measured following Ref. [29], which are summarized in Table 1. Fig. 6b shows the corresponding PL spectrum. From Fig. 6b, it is seen that at 2% green and red co-doping, the PL spectrum is in excellent agreement with the EL spectrum acquired from the full device, which implies that proficient Dexter triplet transfer from the green triplet states to the red triplet states is maintained.

The η_{PL} of the solely red doped film at 4% is indeed higher than that of the 2% red doped film, which is consistent with the lower EL intensity observed in full devices, although the enhancement ratio is not as high as that of the corresponding EL intensity. However, surprisingly, the η_{PL} of the 2% green and red co-doping is lower than the 4% solely red doping yet higher than the 2% solely red doping (see Table 1), which is incommensurate with the EL intensity observed in full devices (see Fig. 3). This suggests that electrical effects by the green phosphors such

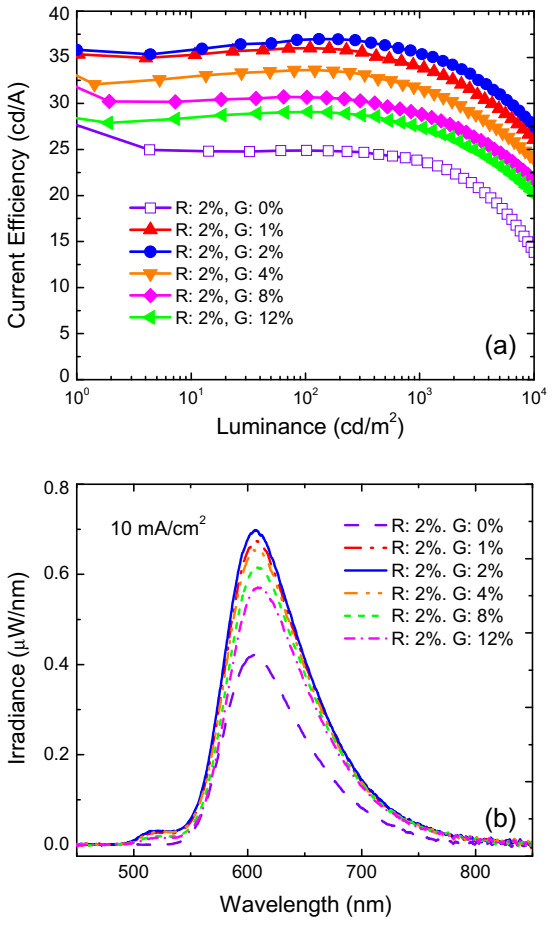

Fig. 2. (a) CE–L plot for selected devices under a fixed red doping and a range of green doping concentrations, and (b) corresponding absolute irradiance spectra at a current density of 10 mA/cm^2.

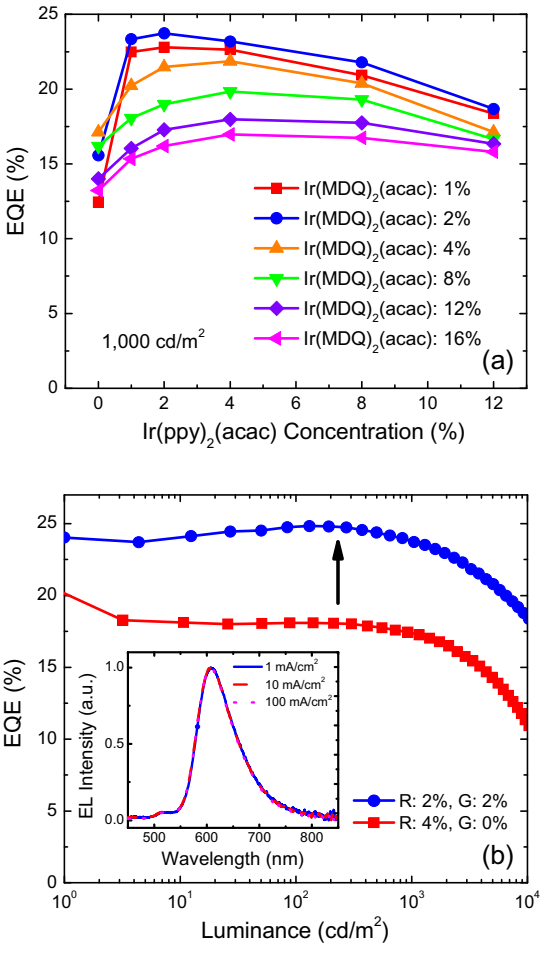

Fig. 3. (a) EQE versus Ir(ppy)$_2$(acac) concentration under a range of Ir(MDQ)$_2$(acac) concentrations at a luminance of 1000 cd/m^2, and (b) EQE versus luminance comparison between the optimized co-doped device and optimized solely red doped device. Inset shows the EL spectra of the optimized co-doped device under a wide range of current densities.

as the carrier trapping could play a critical role. Moreover, we also observed a clear red shift of the PL peak in the 4% solely red doped film in comparison to the co-doped film [see Fig. 6b]. Such a shift is an evidence of aggregation of emitters in the 4% (and higher) solely red doped film, which results in emitter self-quenching. Therefore, we can exclude that the higher EL efficiency in the co-doped (2% each of red and green) device is primarily due to the reduced self-quenching induced by aggregation.

The analysis above implies that the green phosphors do not simply function as a "sensitizer" [30]. It is generally believed that the significantly lower energy gap of the red dopants as compared to the typical host material results in charge trapping and requires higher doping concentrations in order to facilitate charge transport through dopant molecules, which in turn leads to concentration self-quenching and higher driving voltages [10,31–36]. However, in our devices, the current density of the 2% green and red co-doped device is significantly lower than that of the 2% and 4% solely red doped devices as shown in Fig. 7, which suggests that even more charge traps exist in the co-doped device [37,38], yet the efficiency of the co-doped device is considerably higher (see Fig. 2). To further illustrate that the green dopant does function as traps, the driving voltage of the devices at 1 mA/cm^2 is plotted as a function of the green doping concentration in Fig. 7b. At low doping concentrations, the hopping among the green dopants is not preferable and the dopants act mainly as carrier traps, i.e., carrier mobility decreases significantly from 0% to 1% doping concentration which leads to a significant increase in driving voltage (>0.7 V). However, when the doping concentration increases, the hopping among the dopants becomes favorable and the mobility increases as a function of the doping concentration, which leads to a gradual decrease in driving voltage. These results are consistent with the systematic studies shown in Ref. [37].

Moreover, even though the red dopants tend to trap the charges, the excitons are not directly formed on the red dopant but rather in the host at the CBP/TPBi interface and subsequently the energy is transferred to the dopant. This is evidenced by the fact that the turn on voltage of

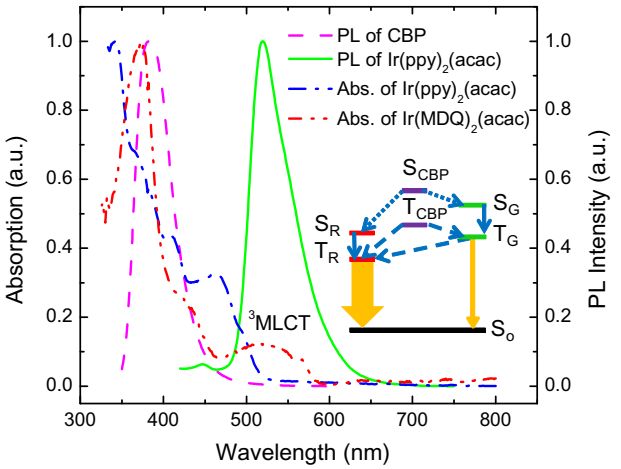

Fig. 4. Normalized absorption spectra of $Ir(ppy)_2(acac)$ and $Ir(MDQ)_2(acac)$ in CH_2Cl_2 (1.0×10^{-5} M), as well as normalized PL spectra of CBP in solid state and $Ir(ppy)_2(acac)$ in CH_2Cl_2 (1.0×10^{-5} M), where the excitation wavelengths are at 330 nm and 400 nm, respectively. Inset illustrates the dominant energy transfer processes between the singlet (S) and triplet (T) energy levels of the host and dopants, where dotted arrows represent Förster transfer, solid arrows denote ISC, and dashed arrows represent Dexter transfer. S_o denotes the ground state.

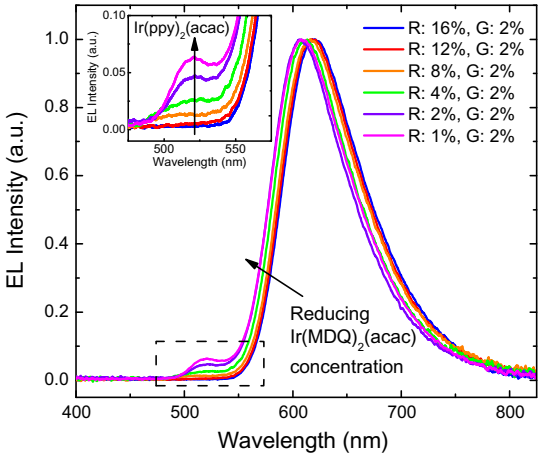

Fig. 5. EL intensity spectra normalized to the dominant red peak at a current density of 10 mA/cm^2 for selected devices under a fixed green doping and a range of red doping concentrations. Inset shows a 10 times magnified spectrum of the region enclosed in the dashed box, which highlights the green spectral peak evolution with $Ir(MDQ)_2(acac)$ concentration reduction.

Table 1
Absolute solid state PL quantum efficiency of organic thin films (100 nm).

Device structure	PL peak (nm)	Quantum efficiency (%)
CBP:R:2%, G:2%	606	73
CBP:R:2%, G:0%	606	70
CBP:R:4%, G:0%	612	77

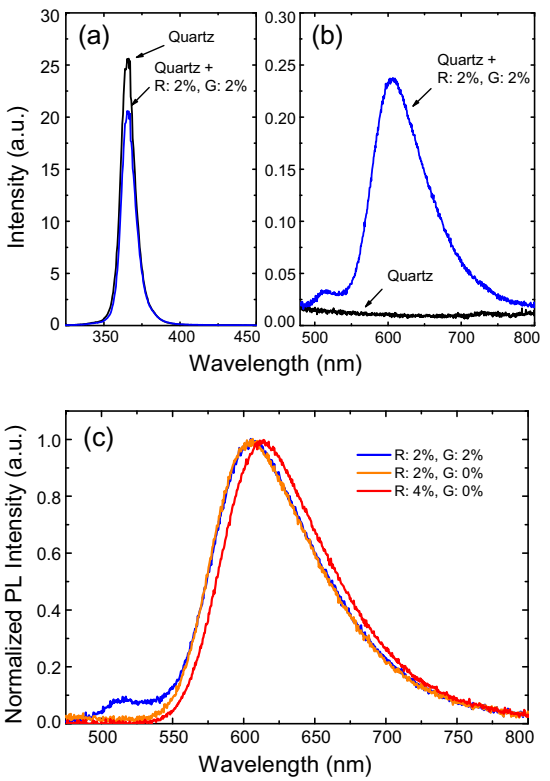

Fig. 6. (a) Excitation intensities and (b) PL spectra of the background (bare quartz substrate) and the CBP thin film (100 nm) doped with 4% $Ir(MDQ)_2(acac)$ on quartz substrate. (c) Normalized PL spectra (after subtraction of the background) of CBP thin film (100 nm) doped with selected concentrations of green and red dopants on a quartz substrate.

3.1 V is significantly higher than the photon energy of the red emission at ~2.05 eV [39]. In the co-doped device, however, the turn on voltage is roughly 0.2 V lower (see the inset of Fig. 7), which indicates that the green phosphors help form excitons [40]. In fact, it has been shown that excitons can be directly formed on $Ir(ppy)_2(acac)$ [25], which is consistent with the results reported herein. It is also worth noting that, as mentioned previously the device structure employed in this study is without any significant barrier or blocking layer, which has been

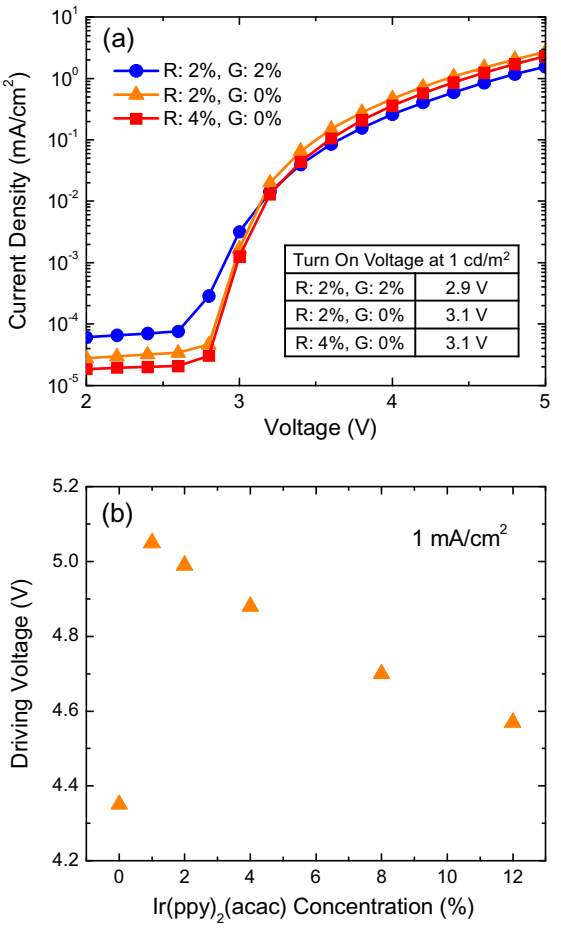

Fig. 7. (a) Current density versus voltage for selected devices. The inset shows a table of turn on voltages defined at a luminance of 1 cd/m^2. (b) Driving voltage versus Ir(ppy)$_2$(acac) doping concentration for devices with 2% red doping at a current density of 1 mA/cm^2.

believed to be necessary to confine the carriers and excitons for high EL efficiency [41–43]. The high performance of the co-doping device suggests that the green phosphors function as carrier traps and exciton forming sites. We can therefore conclude that the green phosphors are able to *harvest* excitons and subsequently perform efficient triplet exciton energy transfer to the red phosphors, thereby enhancing the overall efficiency of the co-doped PHOLED device.

3. Conclusions

In summary, we have realized simplified red PHOLEDs with substantially enhanced efficiency by employing exciton harvesting green molecules that perform efficient Dexter energy transfer from the green triplet states to the red triplet states. Particularly, a maximum current efficiency of 37 cd/A and EQE of 24.8% have been achieved without additional out-coupling enhancements. The efficiency roll-off of the devices is also excellent with a high EQE of 20.8% even at a high luminance of 5000 cd/m^2, which suggests minimal charge carrier accumulation that could trigger various quenching processes. Further, we observe a stable EL spectrum under a wide range of driving conditions, which implies effective triplet exciton confinement in the EML. The application of exciton harvesting molecules followed by efficient energy transfer could spark the development of higher performance OLEDs for full-color displays and solid state lighting.

4. Experimental

All devices were fabricated by thermal evaporation in a Kurt J. Lesker LUMINOS® cluster tool with a base pressure of ~10^{-8} Torr on a glass substrate (1.1 mm thick) that was pre-coated commercially with 120 mm thick indium tin oxide (ITO) having a sheet resistance of 15 Ω/□ . Prior to usage, the substrate was degreased with standard solvents and cleaned in a UV–ozone chamber. The active area of each device (~2 mm^2) was verified with an optical microscope to ensure device-to-device consistency. The deposited layer thickness was monitored by a quartz crystal microbalance calibrated by spectroscopic ellipsometry (Sopra GES 5E). Both Ir(ppy)$_2$(acac) and Ir(MDQ)$_2$(acac) dopants were purified by vacuum sublimation before use to ensure the highest purity attainable.

Current–voltage characteristics were measured using an HP4140B pA meter, and luminance–voltage measurements were carried out using a Minolta LS-110 Luminance Meter. The EL spectra were measured using an Ocean Optics USB4000 spectrometer whereas the luminous flux for the EQE calculation was measured using an integrating sphere equipped with a silicon photodiode with NIST traceable calibration [44]. The solid state and solution PL measurements were conducted using Perkin Elmer LS55 fluorescence spectrometer and the absorption measurements were carried out using Perkin Elmer Lambda 25 UV–vis spectrometer. The absolute quantum yield measurements were carried out in a custom built setup according to the procedure reported in Ref. [29]. A 365 nm collimated LED from Thorlabs (M365L2-C2) is used as the excitation source, which is directed onto the sample consisted of 100 nm thick organic film deposited on 1 mm thick quartz substrate that is mounted inside a calibrated integrating sphere, and the light generated is detected using an Ocean Optics Maya 2000 Pro spectrometer.

Acknowledgment

We would like to acknowledge Natural Sciences and Engineering Research Council (NSERC) of Canada for the funding of this research.

References

[1] H.H. Chou, C.H. Cheng, Adv. Mater. 22 (2010) 2468.
[2] D.H. Kim, N.S. Cho, H.Y. Oh, J.H. Yang, W.S. Jeon, J.S. Park, M.C. Suh, F.H. Kwon, Adv. Mater. 23 (2011) 2721.
[3] S.J. Su, E. Gonmori, H. Sasabe, J. Kido, Adv. Mater. 20 (2008) 4189.
[4] L.X. Xiao, Z.J. Chen, B. Qu, J.X. Luo, S. Kong, Q.H. Gong, J.J. Kido, Adv. Mater. 23 (2011) 926.
[5] S.O. Jeon, S.E. Jang, H.S. Son, J.Y. Lee, Adv. Mater. 23 (2011) 1436.
[6] J.J. Lin, W.S. Liao, H.J. Huang, F.I. Wu, C.H. Cheng, Adv. Funct. Mater. 18 (2008) 485.

[7] Y.T. Tao, Q. Wang, C.L. Yang, C. Zhong, K. Zhang, J.G. Qin, D.G. Ma, Adv. Funct. Mater. 20 (2010) 304.
[8] S.J. Su, C. Cai, J. Kido, Chem. Mater. 23 (2011) 274.
[9] C.-H. Fan, P. Sun, T.-H. Su, C.-H. Cheng, Adv. Mater. 23 (2011) 2981.
[10] J.H. Lee, H.H. Tsai, M.K. Leung, C.C. Yang, C.C. Chao, Appl. Phys. Lett. 90 (2007) 243501.
[11] C.H. Chien, C.F. Shu, F.M. Hsu, Y. Chi, Org. Electron. 10 (2009) 871.
[12] C.L. Yang, Y.T. Tao, Q. Wang, L. Ao, C. Zhong, J.G. Qin, D.G. Ma, J. Mater. Chem. 20 (2010) 1759.
[13] J.H. Jou, S.M. Shen, S.H. Chen, M.H. Wu, W.B. Wang, H.C. Wang, C.R. Lin, Y.C. Chou, P.H. Wu, J.J. Shyue, Appl. Phys. Lett. 96 (2010) 143306.
[14] R. Meerheim, S. Scholz, S. Olthof, G. Schwartz, S. Reineke, K. Walzer, K. Leo, J. Appl. Phys. 104 (2008) 014510.
[15] J.H. Jou, P.H. Wu, C.H. Lin, M.H. Wu, Y.C. Chou, H.C. Wang, S.M. Shen, J. Mater. Chem. 20 (2010) 8464.
[16] M.A. Baldo, C. Adachi, S.R. Forrest, Phys. Rev. B 62 (2000) 10967.
[17] S. Reineke, G. Schwartz, K. Walzer, M. Falke, K. Leo, Appl. Phys. Lett. 94 (2009) 163305.
[18] S. Reineke, K. Walzer, K. Leo, Phys. Rev. B 75 (2007) 125328.
[19] C.H. Cheng, J.P. Duan, P.P. Sun, Adv. Mater. 15 (2003) 224.
[20] Z.B. Wang, M.G. Helander, J. Qiu, D.P. Puzzo, M.T. Greiner, Z.W. Liu, Z.H. Lu, Appl. Phys. Lett. 98 (2011) 073310.
[21] Y. Kawamura, J. Brooks, J.J. Brown, H. Sasabe, C. Adachi, Phys. Rev. Lett. 96 (2006) 017404.
[22] V. Adamovich, M.S. Weaver, M.-H.M. Lu, US Patent, 2010244725 (2007).
[23] Y. Kawamura, K. Goushi, J. Brooks, J.J. Brown, H. Sasabe, C. Adachi, Appl. Phys. Lett. 86 (2005) 071104.
[24] I.C. Chen, K.C. Tang, K.L. Liu, Chem. Phys. Lett. 386 (2004) 437.
[25] C. Adachi, M.A. Baldo, M.E. Thompson, S.R. Forrest, J. Appl. Phys. 90 (2001) 5048.
[26] T. Tsuzuki, S. Tokito, Adv. Mater. 19 (2007) 276.
[27] G.L. Closs, M.D. Johnson, J.R. Miller, P. Piotrowiak, J. Am. Chem. Soc. 111 (1989) 3751.
[28] M.A. Baldo, S.R. Forrest, Phys. Rev. B 62 (2000) 10958.
[29] Y. Kawamura, H. Sasabe, C. Adachi, Jpn. J. Appl. Phys. 43 (2004) 7729.
[30] J.H. Seo, E.Y. Choi, H.M. Kim, Y.K. Kim, S.O. Kim, K.H. Lee, S.S. Yoon, J.T. Je, Mol. Cryst. Liq. Cryst. 538 (2011) 91.
[31] A. Tsuboyama, H. Iwawaki, M. Furugori, T. Mukaide, J. Kamatani, S. Igawa, T. Moriyama, S. Miura, T. Takiguchi, S. Okada, M. Hoshino, K. Ueno, J. Am. Chem. Soc. 125 (2003) 12971.
[32] C.L. Li, Y.J. Su, Y.T. Tao, P.T. Chou, C.H. Chien, C.C. Cheng, R.S. Liu, Adv. Funct. Mater. 15 (2005) 387.
[33] C.H. Cheng, D.K. Rayabarapu, B.M.J.S. Paulose, J.P. Duan, Adv. Mater. 17 (2005) 349.
[34] Y. Chi, Y.L. Tung, S.W. Lee, L.S. Chen, C.F. Shu, F.I. Wu, A.J. Carty, P.T. Chou, S.M. Peng, G.M. Lee, Adv. Mater. 17 (2005) 1059.
[35] H. Kanno, K. Ishikawa, Y. Nishio, A. Endo, C. Adachi, K. Shibata, Appl. Phys. Lett. 90 (2007) 123509.
[36] C.L. Ho, W.Y. Wong, Z.Q. Gao, C.H. Chen, K.W. Cheah, B. Yao, Z.Y. Xie, Q. Wang, D.G. Ma, L.A. Wang, X.M. Yu, H.S. Kwok, Z.Y. Lin, Adv. Funct. Mater. 18 (2008) 319.
[37] S.K. So, W.H. Choi, C.H. Cheung, J. Photon, Energy 1 (2011) 011011.
[38] P.A. Lane, L.C. Palilis, D.F. O'Brien, C. Giebeler, A.J. Cadby, D.G. Lidzey, A.J. Campbell, W. Blau, D.D.C. Bradley, Phys. Rev. B 63 (2000) 235206.
[39] Taken from the peak of the EL spectrum.
[40] Z.B. Wang, M.G. Helander, Z.M. Hudson, J. Qiu, S. Wang, Z.H. Lu, Appl. Phys. Lett. 98 (2011) 213301.
[41] V.I. Adamovich, S.R. Cordero, P.I. Djurovich, A. Tamayo, M.E. Thompson, B.W. D'Andrade, S.R. Forrest, Org. Electron. 4 (2003) 77.
[42] M. Ikai, S. Tokito, Y. Sakamoto, T. Suzuki, Y. Taga, Appl. Phys. Lett. 79 (2001) 156.
[43] S.H. Kim, J. Jang, J.Y. Lee, Appl. Phys. Lett. 90 (2007) 223505.
[44] S.R. Forrest, D.D.C. Bradley, M.E. Thompson, Adv. Mater. 15 (2003) 1043.